

Coherence Dispersion and Temperature Scales in a Quantum-Biology Toy Model

Fernando Parisio*

Departamento de Física, Centro de Ciências Exatas e da Natureza,
Universidade Federal de Pernambuco, Recife, Pernambuco 50670-901 Brazil

In this work, we investigate how quantum coherence can scatter among the several off-diagonal elements of an arbitrary quantum state, defining coherence dispersion (Δ_c). It turns out that this easily computable quantity is maximized for intermediate values of an appropriate entropy, a prevalent signature of complexity quantifiers across different fields, from linguistics and information science to evolutionary biology. By focusing on out-of-equilibrium systems, we use the developed framework to address a simplified model of cellular energetics, involving remanent coherence. Within the context of this model, the precise energy of 30.5 kJ/mol (the yield of ATP-ADP conversion) causes the temperature range where Δ_c is maximized to be compatible with temperatures for which unicellular life is reported to exist. Low levels of coherence suffice to support this conclusion.

INTRODUCTION

Several everyday experiences rely on coherence, such as the interference patterns on the surface of a pond [1] or diffracted sunlight [2]. What challenges common sense and makes quantum coherence unique is that it allows for the coexistence of classically irreconcilable circumstances. This possibility of superposition is not only a cornerstone of quantum phenomena, but also a pervasive ingredient in new technologies. Therefore, it does not come as a surprise the enormous effort invested to characterize quantum coherence [3–11] and relate it with other primeval resources [11–18], in the last decade.

Studies on genuine multi-level coherence [19, 20], or how coherence distributes over separated subsystems [21], e. g., providing a finer characterization, have been carried out more recently. These works illustrate the complexity involved in a deeper description of coherence, beyond its bare quantification.

Although notions related to complexity pervade all scientific disciplines, setting a theoretical framework with operational concepts is still an open problem in many fields. Such framework is well established in certain areas, such as information science, e. g., where quantitative definitions of computational complexity exist. The formalization of complexity has also been explored in a multitude of fields including text analysis [22, 23], ecology [24, 25], and other complex systems [26–28]. A common feature of complexity indicators is their dual relationship with disorder (entropy) [26]. Typically, low complexity is linked with both maximal and minimal entropy, while maximal complexity occurs for intermediate entropy.

In this context, it is natural to consider the dispersion of the coherences of a quantum state, in a given basis. We address this question and, in the first part of this work, propose an easily computable variability figure of merit, which captures essential features of complexity quantifiers, being valid for composite systems with an arbitrary number of components.

An arena where variability may meet systems bearing some level of coherence is the emergent field of quan-

tum biology [29–32]. Biological, thus, out-of-equilibrium systems are open and warm. However, there is growing evidence that quantum coherence may partially survive under certain conditions and scales [33] (see also [34–37]). In the second part of this work we build a model which connects cell energetics with coherence dispersion. The relevant energy scale is assumed to be the gap between adenosine triphosphate (ATP) and adenosine diphosphate (ADP) molecules, the microscopic energy “currency” for all living organisms. Estimates from the literature for the average number of ATP molecules within a typical cell are also employed. We find that coherence dispersion exhibits a peaked maximum for a finite temperature. The position of this maximum varies slowly as the model parameters are changed within several orders of magnitude, providing a robust temperature interval, which nearly coincides with the temperatures for which unicellular life is reported to be viable [38].

COHERENCE DISPERSION

Some well known quantities related to a density matrix can be seen under an alternative but elementary, statistical perspective. Consider an arbitrary orthonormal basis $\{|i\rangle\}$ in a Hilbert space of finite dimension D and a quantum state ϱ in the associated Hilbert-Schmidt space $B(\mathcal{H})$. Let us first address the populations, $\varrho_{ii} = \langle i|\varrho|i\rangle$. The constraint $\text{Tr}(\varrho) = \sum_i \varrho_{ii} = 1$ can be equivalently cast as follows: the mean population is fixed, $\overline{\varrho_{ii}} \equiv \overline{\rho}_p = 1/D$, where the over-score denotes average ($\text{Tr}(\varrho) = 1 \Leftrightarrow \overline{\rho}_p = 1/D$). If, for whatever reason, one calculates an average, the natural next step is to determine the variance (σ^2). In the present case it reads $D\sigma_p^2 = \sum_i (\varrho_{ii} - \overline{\rho}_p)^2$. Interestingly, this is nothing but the squared predictability [39] (apart from a multiplicative factor):

$$P^2 = \sum_{i=1}^D \varrho_{ii}^2 - \frac{1}{D} = D\sigma_p^2,$$

property matrix elements	average	variance
populations	$\frac{1}{D}$	$\frac{P^2}{D}$
coherences	$\frac{C_1}{D^2 - D}$	$\frac{\Delta_c}{D^2 - D}$

FIG. 1: Summary of statistical properties of the entries of ϱ . Eq. (1) fills the gap related to the variance of the absolute values of the coherences.

introduced as a complementary quantity to visibility, in the context of quantum optics.

Now consider the absolute values of the $D^2 - D$ coherences of ϱ . It is evident that the corresponding average $|\varrho_{ij}| \equiv \bar{\rho}_c$, $i \neq j$, is simply proportional to the ℓ_1 norm of coherence:

$$\bar{\rho}_c = \frac{1}{D^2 - D} \sum_{i \neq j}^D |\varrho_{ij}| = \frac{C_1(\varrho)}{D^2 - D},$$

thus being a proper coherence monotone [3]. We are left with the variance of the numbers $|\varrho_{ij}|$ ($i \neq j$), $\sigma_c^2 = \sum_{i \neq j}^D (|\varrho_{ij}| - \bar{\rho}_c)^2 / (D^2 - D) \equiv \Delta_c(\varrho) / (D^2 - D)$, where we call Δ_c the coherence dispersion. We immediately obtain:

$$\Delta_c(\varrho) = C_2(\varrho) - \frac{(C_1(\varrho))^2}{D^2 - D}, \quad (1)$$

with $C_2(\varrho) = \sum_{i \neq j}^D |\varrho_{ij}|^2$ being the so-called ℓ_2 “norm” of coherence. Eq. (1) fills the otherwise blank entry in Fig. 1. Note that $\Delta_c = 0$ for any incoherent state but also for any maximally coherent state. In addition, Δ_c vanishes for the simplest systems: those with $D = 2$. Other properties follow directly from the general features of variances, for instance, convexity [40]: $\Delta_c(\sum_k p_k \varrho_k) \leq \sum_k p_k \Delta_c(\varrho_k)$, see the appendix, where we also show that $0 \leq \Delta_c < 1$, for any dimension D , with the upper bound being approached for D arbitrarily large. So it is not the matter of an extensive quantity.

We note that Δ_c displays other traits of a complexity indicator, due to its relation with an appropriate entropy, namely, the relative entropy of coherence [3]. It is associated with coherences only and given by $S_c(\varrho) = S(\varrho_{\text{diag}}) - S(\varrho)$, where S is the von Neumann entropy and ϱ_{diag} is the incoherent state with the same populations as ϱ . Therefore, for an arbitrary pure state $\psi = |\psi\rangle\langle\psi|$ we have $S_c(\psi) = S(\psi_{\text{diag}})$, since $S(\psi) = 0$.

It is easy to see that, within pure states, one can reach minimal and maximal values of S_c . If the ket is one of the elements of the selected basis, say $|1\rangle$, then $S_c = 0$;

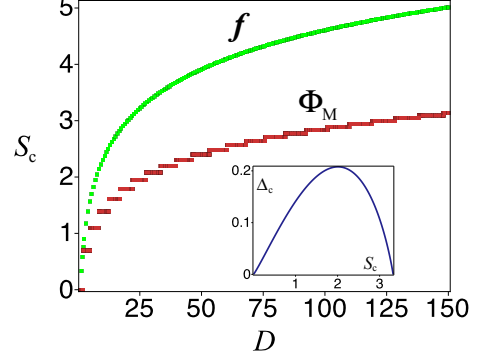


FIG. 2: S_c against the dimension D , for the states f and Φ_M . Inset: Δ_c versus S_c for the state $|\psi_x\rangle\langle\psi_x|$ with $D = 10$. All plotted quantities are dimensionless.

while, for $|f\rangle = (1/\sqrt{D}) \sum_i |i\rangle$ we get $S_c = \log D$. It is immediate that in both cases we obtain $\Delta_c = 0$. Therefore, Δ_c vanishes for maximal and minimal S_c . This is an ubiquitous signature of complexity indicators in a variety of fields [22–28]. In addition, complexity figures of merit attain a single maximum at a some intermediate entropy value. Due to convexity, it is clear that states which maximize Δ_c must be pure ($|\Phi_M\rangle$). Indeed, it is always possible to express an arbitrary state ϱ in terms of a convex sum of pure states, $\varrho = \sum p_i |\varphi_i\rangle\langle\varphi_i|$. From convexity, $\Delta_c(\varrho) \leq \sum_i p_i \Delta_c(\varphi_i)$ and $\Delta_c(\varphi_i) \leq \Delta_c(\Phi_M)$, by hypothesis. Therefore, $\Delta_c(\varrho) \leq \Delta_c(\Phi_M)$, for any non-pure ϱ . In the appendix we show that the maximum-dispersion states assume the form:

$$|\Phi_M\rangle = r(D)^{-1/2} \sum_{i=1}^{r(D)} |i\rangle,$$

where $r(D) < D$ is an involved integer function of the dimension D [e.g., $r(3) = r(4) = 2$, $r(10) = 4$, and $r(100) = 17$]. These states present intermediate entropy of coherence, $S_c(\Phi_M) = \log r(D)$, as can be seen in Fig. 2 in comparison with maximal-entropy states f , with $S_c(f) = \log D$.

This behavior is not limited to states with maximum dispersion. Consider the family of normalized states $|\psi_x\rangle = a(x)|1\rangle + b(x) \sum_{i>1} |i\rangle$, with $a(x) = 1 - x$, $b(x) = \sqrt{\frac{x(2-x)}{D-1}}$, which interpolates between $|1\rangle$ ($x = 0$) and $|f\rangle$ ($x = 1$), as x goes from 0 to 1. The state ψ_x never coincides with Φ_M , but as we vary x , some constrained maximum-dispersion state is attained, as shown in the inset of Fig. 2. The curve shows the archetypical dependence of complexity-entropy diagrams [22–28].

Complexity is often an emergent property and it would be interesting to express the dispersion of a composite system comprising a large number of subsystems. We now show that Δ_c is also computable in this sense: one can easily determine $\Delta_c(\rho^{\otimes n})$, for any number of copies

n , from quantities easily obtainable from a single copy.

It turns out that Δ_c can be completely expressed in terms of 1-scalable quantities [41], namely, P^2 , C_1 , and the purity $\Pi \equiv \text{Tr}(\rho^2)$. This is done by employing the complementarity relation [42],

$$C_2 + P^2 - \Pi + \frac{1}{D} = 0$$

to eliminate C_2 , which is not scalable [43]. Explicitly, for $\varrho = \rho^{\otimes n}$ we have: $P^2(\rho^{\otimes n}) = (P(\rho)^2 + 1/d)^n - 1/d^n$, $\Pi(\rho^{\otimes n}) = [\Pi(\rho)]^n$, and $C_1(\rho^{\otimes n}) = (1 + C_1(\rho))^n - 1$, where ρ is represented by a $d \times d$ matrix, so $D = d^n$. The expression for the multi-copy ℓ_1 norm of coherence is given in [43]. The remaining results are derived in the appendix and the n -copy coherence dispersion reads:

$$\Delta_c(\rho^{\otimes n}) = \Pi^n - \left(P^2 + \frac{1}{d} \right)^n - \frac{[(1 + C_1)^n - 1]^2}{d^{2n} - d^n}, \quad (2)$$

where $\Pi \equiv \Pi(\rho)$, $P \equiv P(\rho)$, and $C_1 \equiv C_1(\rho)$. The result is indeed more general. Consider the state $\varrho = \rho^{(1)} \otimes \rho^{(2)} \otimes \dots \otimes \rho^{(n)}$, satisfying $\rho_{ij}^{(k)} = e^{\phi_{k\ell}} \rho_{ij}^{(\ell)}$, where $\phi_{k\ell}$ are arbitrary phases and $k, \ell \in \{1, \dots, n\}$. Then, since Π , P , and C_1 only depend on the absolute values of the matrix entries, it follows that $V(\rho^{(1)} \otimes \rho^{(2)} \otimes \dots \otimes \rho^{(n)}) = V(\rho^{(1)}^{\otimes n})$. So, if the states differ by local phases, Eq. (48) can still be used. The same conclusion holds for states that differ by arbitrary permutations of the basis elements. Note also that coherence dispersion can be super-activated. A simple instance is as follows: any two-qubit state σ has $\Delta_c(\sigma) = 0$, but we usually have $\Delta_c(\sigma^{\otimes n}) \neq 0$, for $n > 1$.

COHERENCE DISPERSION AND ATHERMALITY

To complete the tools needed to develop the model of the next section, we investigate how Δ_c relates to thermodynamics. Consider a system in thermal equilibrium with a reservoir at absolute temperature T . It is described by

$$\rho_G(T) = \frac{1}{Z} \sum_i e^{-E_i/k_B T} |i\rangle\langle i|,$$

where Z is the canonical partition function, k_B is the Boltzmann constant, and $\{|i\rangle\}$ is the energy basis, which also plays a central role in the resource theory of athermality [44]. Since the Gibbs state has no coherences, we simply obtain $\Delta_c(\rho_G) = 0$. Also, incoherent states with populations that deviate from the Maxwell-Boltzmann (MB) distribution have zero dispersion. We say that these states display *classical athermality*.

Of course, Δ_c can only appear in states with non-zero coherences, thus, being out of equilibrium in a

quantum sense. One class that is particularly interesting is that of coherent Gibbs states [45], given by $|\Psi_G\rangle = \frac{1}{\sqrt{Z}} \sum_i e^{-E_i/2k_B T} |i\rangle$, which, under full decoherence, becomes ρ_G . We intend to use these states to describe microscopic open systems, which are in contact with a thermal bath, but not in equilibrium with it.

A pure state is a contrived assumption for an open system. We, thus, consider partially coherent Gibbs states:

$$G = \lambda |\Psi_G\rangle\langle \Psi_G| + (1 - \lambda) \rho_G. \quad (3)$$

Note that, since the populations obey the MB distribution, these states present pure quantum athermality. In this case, the single-copy coherence dispersion can be compactly expressed as (see the appendix):

$$\Delta_c(G(T)) = \lambda^2 (1 - \Pi_{\text{eq}}(T)) - \frac{\lambda^2}{d^2 - d} (1 - 1/\Pi_{\text{eq}}(2T))^2,$$

where $\Pi_{\text{eq}}(T)$ is the purity of the thermal-equilibrium Gibbs state. The dispersion $\Delta_c(G(T))$ of the non-equilibrium system in contact with a reservoir at temperature T , depends on the purity associated with the corresponding equilibrated system at two different temperatures, a signature of athermality. Notice that λ^2 is a global multiplicative factor, in particular, not affecting the location of extremal points, whenever they exist.

In the appendix we show that the corresponding n -copy coherence dispersion is given by:

$$\Delta_c(G^{\otimes n}(\tau)) = (\lambda^2 + (1 - \lambda^2)\Pi_{\text{eq}}(T))^n - \Pi_{\text{eq}}(T)^n - \frac{1}{d^{2n} - d^n} ((1 - \lambda + \lambda/\Pi_{\text{eq}}(2T))^n - 1)^2 \quad (4)$$

Hereafter we will focus on d -level systems. In the appendix we derive an expression for Δ_c for n such systems, which can exchange energy with the bath in packets of energy ϵ , i. e., $E_j = j\epsilon$, $j = 1 \dots, d$, implying

$$\Pi_{\text{eq}}(\tau) = \tanh\left(\frac{2}{\tau}\right) \coth\left(\frac{2d}{\tau}\right),$$

where τ is the dimensionless temperature given by $\tau = 4k_B T/\epsilon$. By plugging this input in Eq. (49) we find a distinctive property: Δ_c presents a single, sharp global maximum at a finite temperature τ^* .

We thus reached an expression for coherence dispersion of an out-of-equilibrium system comprised by an arbitrary number of elementary entities. The system is in contact with an environment at absolute temperature T , and, importantly, bear some remanent level of coherence, λ . Living structures are non-equilibrium systems par excellence (full equilibration with the environment meaning death) and it is believed that some microscopic reactions, relevant in quantum biology, rely on partial coherence [30, 36, 37]. Thus, microscopic processes in biology are a natural terrain where variability, athermality, and coherence may appear together.

CELLULAR ENERGETICS AND QUANTUM AETHERMALITY: A TOY MODEL

Our goal is to investigate how coherence, even if residual, may manifest in cell energetics, through a two-level toy model. We will assume that each two-level system represents an individual energy-consumption site (ECS) within a unicellular organism. These sites may represent a channel for active transport or a DNA base pair being unwinded, for instance. So, we will not make any distinction among the several possible uses of the available energy. The elementary process in cell energetics is the ubiquitous biochemical cycle of ATP hydrolysis, producing an ADP molecule plus an inorganic phosphate group (P_i), and releasing a large amount of energy (~ 30.5 kJ per mol). We set the energy gap between the two levels as the energy difference between single ATP and ADP molecules, $\epsilon \approx 0.316$ eV. Further, we assume that the ECSs can be active (\star) or inactive (\circ), or in a superposition, and, without loss of generality, we set $\epsilon_\circ = 0$ and $\epsilon_\star \equiv \epsilon$.

In thermodynamic equilibrium, the state of a statistical ensemble describing this system would be the simplest instance of the Gibbs state $\rho_G = (|\circ\rangle\langle\circ| + e^{-\frac{1}{kT}}|\star\rangle\langle\star|)/\mathcal{Z}$, where the thermal bath is provided by the medium in which the cell is immersed, with the absolute temperature given by

$$T = \tau\epsilon/4k_B \approx \tau \times 917 \text{ K.} \quad (5)$$

In the opposite regime, the pure quantum superposition, and thus, unrealistic for an open system, is $|\Psi_G\rangle = (|\circ\rangle + e^{-\frac{1}{8\tau}}|\star\rangle)/\sqrt{\mathcal{Z}}$, where the Born probabilities are constrained to coincide with those of MB, so that we only have quantum athermality. To consider some level of coherence a state like (3) will be used in our model. Given that the system is warm and open we may assume that strong phase damping takes place. The results presented in what follows are remarkably robust against decoherence.

Crucially, we need to estimate the number n of ECSs participating with finite coherence, at any moment, on average. To do that we consider the well-studied bacterium *E. Coli*, which is able to grow in the approximate temperature range $7^\circ\text{C} \lesssim T \lesssim 50^\circ\text{C}$ [46], which, via Eq. (5), corresponds to the narrow interval $0.30 \lesssim \tau \lesssim 0.35$. We now investigate the hypothesis that this temperature interval corresponds to the values spanned by τ^* , the temperature of maximum Δ_c . This association leads to correspond to $300.000 \geq n \geq 50.000$, which is quite compatible with the estimate for the total number of ATP molecules within *E. Coli*, $\mathcal{N} \approx 3 \times 10^6$ [47], which is of the same order of the estimate from the Bionumbers initiative [48], $\mathcal{N}' \approx 1.75 \times 10^6$. It is reasonable to suppose that n is upper bounded by the number \mathcal{N} of ATP molecules within the cell, at any moment ($n < \mathcal{N}$). For definiteness

we use the estimate of [47]. Indeed, our values of n are between 2% and 10% of \mathcal{N} . Our main conclusions would be the same had we used \mathcal{N}' .

Since these figures can strongly vary for different unicellular organisms, in order to include other kinds of cell, we consider values of n one order of magnitude below (above) the lower (higher) value for *E. Coli*. Thus, we consider the broad window $5.000 \leq n \leq 3 \times 10^6$, covering nearly three orders of magnitude. In addition, we use the wide interval of coherence level: $0.001 \leq \lambda \leq 0.3$. Remarkably, the value of τ^* is weakly dependent on n and fairly insensitive to λ . In addition, it might be argued that several essential processes in cell energetics make use of more than a single ATP molecule. For this reason, we considered ECSs with dimensions $2 \leq d \leq 20$ (see the appendix). Indeed, by varying these parameters within the prescribed intervals, the value of τ^* drifts from 0.257 to 0.434 (mainly due to the variation of n), which, according to Eq. (5), corresponds to the temperature window [236K, 398K] or

$$-37^\circ\text{C} \lesssim T^* \lesssim 125^\circ\text{C}. \quad (6)$$

Of course, the exact limiting temperatures above are of little relevance, given the approximations involved. What is to be remarked is the fact that (6) tightly contains the temperature interval for which unicellular life is reported to be sustainable, $-20^\circ\text{C} \lesssim T_{\text{life}} \lesssim 122^\circ\text{C}$ [38, 49, 50]. In marked contrast with the weak dependence on n , and insensitivity to d , and λ , the position of the maximum of Δ_c is clearly dependent on the exact value of ϵ . If, e. g., one increases the energy by a factor of two, the corresponding window becomes [472K, 796K], or $199^\circ\text{C} \lesssim T^* \lesssim 523^\circ\text{C}$, totally incompatible with life. Thus, the exact ATP-ADP energy difference plays a sensitive role. In Fig. 3 we plot of Δ_c against n and τ . It vanishes in the light gray region and the green stripe marks the locus of the maxima. The larger bar between the dashed lines gives the temperature interval (6), while the shorter bar gives the temperature interval for which unicellular life occurs [38]. In the appendix we display several other plots illustrating the properties described here.

There is no reason for all ECS to have real coherences, but, due to the observation after Eq. (48), the results remain valid for random phases. In addition, the fact that we consider all coherent ECS's to have the same coherence level, is justified by interpreting λ as an effective, average parameter. What about the incoherent fraction of ECSs? In the final part of the appendix we consider a more general model, incorporating the fraction of ECSs which are in thermal states, constituting an “incoherent buffer”. In this case the state of the system is $G^{\otimes n} \otimes \rho_G^{\otimes(N-n)}$, where N is the total number of ECSs within the cell. In spite of a qualitative change in the contour plots (the relevant parameter is N rather than n), we find a very similar temperature window as we go

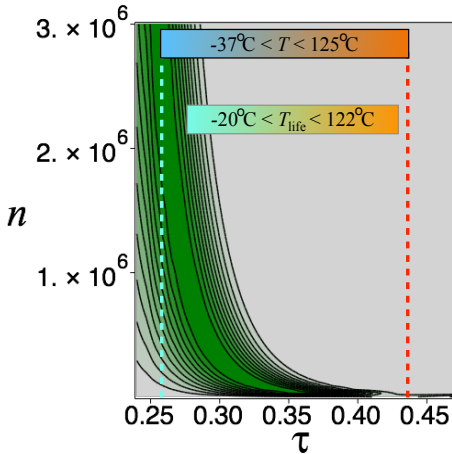


FIG. 3: Δ_c as a function of τ and n (starting from 5000) for $\lambda = 0.1$. The contours are essentially the same for any value of $\lambda \in [0.001, 0.3]$ and for $d = 2, \dots, 20$.

from $N = 5000$ to $N = 3 \times 10^6$. For each value of N we vary n from 5000 to N .

FINAL REMARKS

It is a tenable position to assume that in the course of evolution nature learnt to make use of quantum phenomena to promote fitness [30]. Yet, a common criticism raised against the existence of quantum effects in biology is the inevitable occurrence of decoherence. The fact that our findings remain valid for very low levels of coherence may offer a distinct argument in favor of quantum effects in biological systems.

Despite the simplicity of the described models, the fact that the interval (6) contains the whole range of temperatures in which unicellular life occurs, should motivate further studies on coherence dispersion in quantum biology. One clearly interesting question is: Does the environment temperature exert any kind of evolutionary pressure over the microscopic energy scale that is ultimately selected by the microorganisms?

In addition, the concepts developed here should play some role in quantum foundations and information. In this context, it would be interesting to know whether a formal resource-theoretical framework can be set for coherence dispersion.

The author thanks P. R. A. Campos and M. Copelli for their comments and suggestions on this work. This research received financial support from the Brazilian agencies Coordenação de Aperfeiçoamento de Pessoal de Nível Superior (CAPES), Conselho Nacional de Desenvolvimento Científico e Tecnológico (CNPq), Fundação de Amparo à Pesquisa do Estado de São Paulo (FAPESP - Grant 2021/06535-0), and Fundação de Am-

paro à Ciéncia e Tecnologia do Estado de Pernambuco (FACEPE - Grant BPP-0037-1.05/24).

* fernando.parisio@ufpe.br

- [1] W. H. Knox, M. Alonso and E. Wolf, *Spatial coherence from ducks*, Phys. Today, 11 (2010).
- [2] N. Abas, A. R. Kalair, and M. S. Saleem, Results Eng. **23**, 102471 (2024).
- [3] T. Baumgratz, M. Cramer, and M. B. Plenio, Phys. Rev. Lett. **113**, 140401 (2014).
- [4] D. Girolami, Phys. Rev. Lett. **113**, 170401 (2014).
- [5] X. Yuan, H. Zhou, Z. Cao, and X. Ma, Phys. Rev. A **92**, 022124 (2015).
- [6] C. Napoli, T. R. Bromley, M. Cianciaruso, M. Piani, N. Johnston, and G. Adesso, Phys. Rev. Lett. **116**, 150502 (2016).
- [7] S. Rana, P. Parashar, and M. Lewenstein, Phys. Rev. A **93**, 012110 (2016).
- [8] K. Bu, U. Singh, S.-M. Fei, A. K. Pati, and J. Wu, Phys. Rev. Lett. **119**, 150405 (2017).
- [9] J. Xu, L.-H. Shao, and S.-M. Fei, Phys. Rev. A **102**, 012411 (2020).
- [10] G. Biswas, S. Sarkar, A. Biswas, and U. Sen, New J. Phys. **25**, 083030 (2023).
- [11] A. Streltsov, G. Adesso, and M. B. Plenio, Rev. Mod. Phys. **89**, 041003 (2017).
- [12] A. Streltsov, U. Singh, H. S. Dhar, M. N. Bera, and G. Adesso, Phys. Rev. Lett. **115**, 020403 (2015).
- [13] H. Zhu, Z. Ma, Z. Cao, S.-M. Fei, and V. Vedral, Phys. Rev. A **96**, 032316 (2017).
- [14] X. Qi, T. Gao, and F. Yan, J. Phys. A: Math. Theor. **50**, 285301 (2017).
- [15] X. Hu, A. Milne, B. Zhang, and H. Fan, Sci. Rep. **6**, 19365 (2016).
- [16] D.-D. Dong, X.-K. Song, X.-G. Fan, L. Ye, and D. Wang, Phys. Rev. A **107**, 052403 (2023).
- [17] M.-L. Hu, X.-M. Wang, and H. Fan, Phys. Rev. A **98**, 032317 (2018).
- [18] Z.-Y. Ding, H. Yang, H. Yuan, D. Wang, J. Yang, and L. Ye, Phys. Rev. A **100**, 022308 (2019).
- [19] M. Ringbauer, T. R. Bromley, M. Cianciaruso, L. Lami, W. Y. S. Lau, G. Adesso, A. G. White, A. Fedrizzi, and M. Piani, Phys. Rev. X **8**, 041007 (2018).
- [20] T. Giordani, C. Esposito, F. Hoch, G. Carvacho, D. J. Brod, E. F. Galvão, N. Spagnolo, and F. Sciarrino, Phys. Rev. Research **3**, 023031 (2021).
- [21] C. Radhakrishnan, M. Parthasarathy, S. Jambulingam, and T. Byrnes, Phys. Rev. Lett. **116**, 150504 (2016).
- [22] W. Li, Complex Syst. **5**, 381 (1991).
- [23] V. A. Gromov, Q. N. Dang, A. S. Kogan, A. Yerbolova, PeerJ Comput. Sci. **10**, e2550 (2024).
- [24] S. Sippel, H. Lange, M. D. Mahecha, M. Hauhs, P. Bodesheim, T. Kaminski, F. Gans, and O. A. Rosso, PLoS ONE **11**: e0164960. (2016).
- [25] J. G. Colonna, J. R. H. Carvalho, and O. A. Rosso, PLoS ONE **15**, e0229425 (2020).
- [26] T. Hogg and B. A. Huberman, Physica D **22**, 376 (1986).
- [27] M. Zanin and F. Olivares, Comm. Phys. **4**, 190 (2021).
- [28] J. E. Borovsky and A. Osmane, Nonlin. Proc. Geophys. **26**, 429 (2019).

[29] M. Arndt, T. Juffmann, V. Vedral, HFSP Journal **3**, 386 (2009).

[30] S. F. Huelga and M. B. Plenio, Contemp. Phys. **54**, 181 (2013).

[31] A. Marais, B. Adams, A. K. Ringsmuth, M. Ferretti, J. M. Gruber, R. Hendrikx, M. Schuld, S. L. Smith, I. Sinayskiy, T. P. J. Krüger, F. Petruccione, and R. van Grondelle, J. R. Soc. Interface **15**, 20180640 (2018).

[32] C. Aiello, Physics **16**, 79 (2023).

[33] N. Lorenzoni, T. Lacroix, J. Lim, D. Tamascelli, S. F. Huelga, M. B. Plenio, Sci. Adv. **11**, 6751 (2025).

[34] V. Salari, J. Tuszyński, M. Rahnama, and G. Bernroider, J. Phys.: Conf. Ser. **306** 012075 (2011).

[35] G. Di Pietra, V. Vedral, C. Marletto, Sci. Rep. **14**, 20094 (2024).

[36] F. D. Fuller, J. Pan, A. Gelzinis, V. Butkus, S. S. Senlik, D. E. Wilcox, C. F. Yocom, L. Valkunas, D. Abramavicius, and J. P. Ogilvie, Nature Chem. **6**, 706?711 (2014).

[37] R. L. Purchase and H. J. M. Groot, Interface Focus **5**: 20150014 (2015).

[38] A. Clarke, Int. J. Astrobiology **13**, 141 (2014).

[39] D. M. Greenberger and A. Yasin, Phys. Lett. A **128**, 391 (1988).

[40] An Introduction to Convexity, Geir Dahl (2010).

[41] F. Parisio, Phys. Rev. A **102**, 012413 (2020).

[42] M. Jakob and J. A. Bergou, Phys. Rev. A **76**, 052107 (2007).

[43] L. F. Melo and F. Parisio, Quantum Inf. Process. **20**, 355 (2021).

[44] F. G. S. L. Brandão, M. Horodecki, J. Oppenheim, J. M. Renes, and R. W. Spekkens, Phys. Rev. Lett. **111**, 250404 (2013).

[45] M. Lostaglio, D. Jennings, and Terry Rudolph, Nature Commun. **6**, 6383 (2015).

[46] <https://www.who.int/news-room/fact-sheets/detail/e-coli>

[47] R. Phillips and R. Milo, PNAS **106**, 21465 (2009).

[48] R. Milo, P. Jorgensen, and M. Springer, ID 100143, <https://bionumbers.hms.harvard.edu>.

[49] O. Geiges, Adv. Space Res. **18**, 109 (1996).

[50] K. Takai, K. Nakamura, T. Toki, U. Tsunogai, M. Miyazaki, J. Miyazaki, H. Hirayama, S. Nakagawa, T. Nunoura, K. Horikoshi, Proc. Natl. Acad. Sci. USA, **105**, 10949 (2008).

Convexity of Δ_c

For completeness, we give a proof of the convexity of

$$\Delta_c = C_2 - \frac{C_1^2}{D^2 - D}. \quad (7)$$

To unclutter notation with the following vectorization. Let $\mathbf{x} = (|\varrho_{12}|, |\varrho_{13}|, \dots, |\varrho_{1D}|, |\varrho_{23}|, |\varrho_{24}|, \dots, |\varrho_{(D-1)D}|) \in \mathcal{UC}_M \subset \mathbb{R}^M$, with $M = (D^2 - D)/2$ (the number of above-diagonal coherences). The set \mathcal{UC}_M is the M -dimensional unit cube ($0 \leq x_i \leq 1$). With this we simply have $C_1(\varrho) = C_1(\mathbf{x}) = 2 \sum_{j=1}^M x_j$ and $C_2(\varrho) = C_2(\mathbf{x}) = 2 \sum_{j=1}^M x_j^2$. Therefore,

$$\Delta_c(\mathbf{x}) = 2 \sum_{j=1}^M x_j^2 - \frac{4}{D^2 - D} \left(\sum_{j=1}^M x_j \right)^2. \quad (8)$$

Note that the domain of definition of $\Delta_c(\mathbf{x})$ is convex since, $p\mathbf{x} + (1-p)\mathbf{y} \in \mathcal{UC}_M$ for any pair $\mathbf{x}, \mathbf{y} \in \mathcal{UC}_M$. Of course Δ_c is a twice-differentiable function of its argument and the corresponding Hessian matrix $\mathbf{H} = \nabla^2 \Delta_c(\mathbf{x})$ is well defined. Under these conditions, if all minor determinants of \mathbf{H} are non-negative, then Δ_c is convex. Explicitly, the entries of \mathbf{H} are given by

$$H_{ij} = \frac{\partial^2}{\partial x_i \partial x_j} \Delta_c(\mathbf{x}) = 4[\Delta_c]_{ij} - \frac{8}{D^2 - D}. \quad (9)$$

One can easily show that the minor determinant of degree k is

$$\text{Det}_k = 4^k \left(1 - \frac{2k}{D^2 - D} \right) = 4^k \left(1 - \frac{k}{M} \right),$$

which is always non-negative, since $D \geq 2$. This finishes the proof.

Note that for $D = 2$ we have $\text{Det}_k = 0$ for all $k = 1, \dots, M$, which is consistent with the fact that $\Delta_c = 0$ for all 2×2 states. For $D \geq 3$ we have $\text{Det}_k > 0$ for $k = 1, \dots, M-1$ and $\text{Det}_M = 0$. Therefore, we have convexity but not strict convexity. This is also expected because $\Delta_c = 0$ for all states for which all coherences have the same absolute value.

States that maximize Δ_c

Here we determine the general states which maximize coherence dispersion. Thanks to the convexity of Δ_c one can restrict the search to pure states. If the pure state is of rank 1 in the computational basis, then $\Delta_c = 0$ and, thus, no such a state can maximize the dispersion. Next, consider rank-2 states, say $|\psi\rangle = \alpha|1\rangle + \beta|2\rangle + 0(|3\rangle + \dots + |d\rangle)$ and ask which of these states maximize Δ_c . The average of the absolute values of the coherences is

$$\bar{\rho}_c = \frac{2xy}{D^2 - D}, \quad (10)$$

with $x = |\alpha| \neq 0$ and $y = |\beta| \neq 0$. Since we have $D^2 - D - 2$ vanishing coherences, the dispersion reads

$$\Delta_c = (D^2 - D - 2)\bar{\rho}_c^2 + 2(xy - \bar{\rho}_c)^2. \quad (11)$$

Using Eq.(10), we get

$$\Delta_c = 2xy \left(1 - \frac{2}{D^2 - D} \right), \quad (12)$$

which, for $D > 2$, is maximized for $x = y = 1/\sqrt{2}$. In this simple case we were able to deal with the normalization constraint by inspection. So the rank-2 state that maximizes Δ_c in a Hilbert space of arbitrary dimension $D > 2$ is of the kind

$$|\psi\rangle = \frac{1}{\sqrt{2}}(|i\rangle + e^{i\varphi}|j\rangle), \quad (13)$$

with $i \neq j \in \{1, 2, \dots, D\}$ and $\varphi \in [0, 2\pi)$.

Arbitrary rank

We now address the general situation of a pure state of fixed rank r , with $2 < r \leq D$. We write

$$|\psi\rangle = \sum_{i=1}^r \alpha_i |i\rangle, \quad (14)$$

and define $x_i = |\alpha_i|$, with $i \in \{1, 2, \dots, r\}$ and $x_i \neq 0$ (otherwise the rank would differ from r). There are $r^2 - r$ non-vanishing coherences with $|\rho_{ij}| = x_i x_j$. The average of the absolute values of coherences is

$$\bar{\rho}_c = \frac{1}{D^2 - D} \sum_{i \neq j}^r x_i x_j, \quad (15)$$

and the dispersion becomes

$$\Delta_c = (D^2 - D - r^2 + r)\bar{\rho}_c^2 + \sum_{i \neq j}^r (x_i x_j - \bar{\rho}_c)^2. \quad (16)$$

The normalization constraint is given by $\sum_i x_i^2 = 1$. We can deal with this condition via a Lagrange multiplier, so that the function to be maximized is

$$\mathcal{L} = (D^2 - D - r^2 + r)\bar{\rho}_c^2 + \sum_{i \neq j}^r (x_i x_j - \bar{\rho}_c)^2 - \lambda \left(\sum_{i=1}^r x_i^2 - 1 \right). \quad (17)$$

By noting that

$$\frac{\partial \bar{\rho}_c}{\partial x_k} = \frac{2}{D^2 - D} (\Sigma - x_k), \quad \Sigma \equiv \sum_{i=1}^r x_i, \quad (18)$$

after some algebra, the r extremization conditions $\partial\mathcal{L}/\partial x_k = 0$ can be set in the simple form

$$1 + \bar{\rho}_c - \frac{\lambda}{2} = x_k^2 + \frac{\bar{\rho}_c \Sigma}{x_k} \quad (19)$$

for $k = 1, 2, \dots, r$. Since the left-hand side of the above equation is a constant, it must be true that

$$x_k^2 + \frac{\bar{\rho}_c \Sigma}{x_k} = x_j^2 + \frac{\bar{\rho}_c \Sigma}{x_j} \Rightarrow (x_k - x_j) \left(x_k + x_j - \frac{\bar{\rho}_c \Sigma}{x_j x_k} \right) = 0 \quad (20)$$

for all pairs (k, j) . Therefore, either $x_k = x_j$, or

$$x_k + x_j - \frac{\bar{\rho}_c \Sigma}{x_j x_k} = 0 \Rightarrow x_j x_k (x_k + x_j) = \bar{\rho}_c \Sigma. \quad (21)$$

However, since $\bar{\rho}_c \Sigma$ is a constant, this should imply

$$x_j x_k (x_k + x_j) = x_n x_k (x_k + x_n) \Rightarrow x_j^2 - x_n^2 = x_k (x_n - x_j) \Rightarrow x_j + x_n = -x_k, \quad (22)$$

which is impossible, since $x_i > 0$, leading to a contradiction.

Therefore, the only solution is $|\alpha_1| = |\alpha_2| = \dots = |\alpha_r| \equiv x$. Finally, the last condition $\partial\mathcal{L}/\partial\lambda = 0$ is simply normalization: $rx^2 = 1$, or $x = 1/\sqrt{r}$. The Lagrange multiplier is given by

$$\lambda = 2 \frac{(r-1)}{r} \left(1 - \frac{(r^2-r)}{D^2-D} \right). \quad (23)$$

We conclude that, fixed a rank r , with $2 < r < D$, the pure state that maximizes Δ_c is given by

$$|\psi\rangle = \frac{1}{\sqrt{r}} \sum_{j=1}^r e^{i\varphi_j} |j\rangle, \quad (24)$$

with $\varphi_i \in [0, 2\pi)$. Of course, any shuffling of basis elements in the ket above leads to a state that also maximizes the dispersion.

Finding the optimal rank

We are left with the simpler problem of finding the rank that globally maximizes the dispersion, given the dimension D . For a fixed dimension D , the coherence dispersion of the non-full rank states derived in the previous section reads

$$\Delta_c(r) = (D^2 - D - r^2 + r) \bar{\rho}_c^2 + (r^2 - r) \left(\frac{1}{r} - \bar{\rho}_c \right)^2 = \left(1 - \frac{1}{r} \right) \left(1 - \frac{r^2 - r}{D^2 - D} \right), \quad (25)$$

where we used $\bar{\rho}_c = (r-1)/(D^2 - D)$. Note that the above expression vanishes for both, $r = 1$ and $r = D$. We see that $0 \leq \Delta_c \leq 1$, where the upper limit is not tight for any finite D . In fact, we will see that the optimal rank is a slowly increasing function of D , so that, only when the dimension becomes arbitrarily large, we have $\Delta_c \rightarrow 1$, for the maximal state.

By setting $r \rightarrow s$ and treating s as a continuous variable in this intermediate step, one can require $d\Delta_c/ds = 0$, leading to the simple cubic equation

$$s^3 - s^2 = \frac{D^2 - D}{2}, \quad (26)$$

which has a single real root, given by

$$s = \frac{1}{3} \left(1 + \frac{\xi}{2} + \frac{2}{\xi} \right), \quad (27)$$

where

$$\xi = \left(8 + 54(D^2 - D) + 6\sqrt{(D^2 - D)[15 + 81(D - 1/2)^2]} \right)^{1/3}. \quad (28)$$

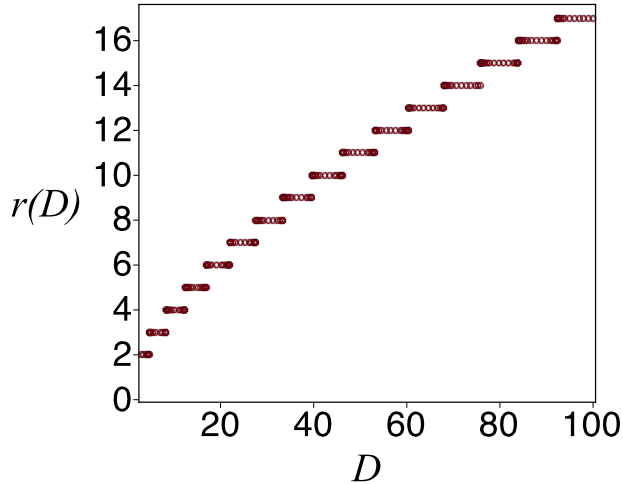


FIG. 4: Rank $r(D)$ which maximizes Δ_c as a function of D .

The optimal (integer) rank $r(D)$ is the neighboring integer to s which maximizes Δ_c . One write the closest smaller integer as $\lfloor s \rfloor$ and the closest larger integer as $\lceil s \rceil$. Using equation (25) we get the following difference

$$\Delta_c(\lceil s \rceil) - \Delta_c(\lfloor s \rfloor) = \frac{1}{\lceil s \rceil \lfloor s \rfloor} - \left(\frac{\lceil s \rceil + \lfloor s \rfloor}{D^2 - D} \right) + \frac{2}{D^2 - D} \equiv X. \quad (29)$$

This quantity oscillates between positive and negative values as s varies. Therefore, one can express the optimal rank $r(D)$ as

$$r(D) = \lfloor s \rfloor + \frac{1 + \text{sign}(X)}{2}, \quad (30)$$

which is a slowly increasing function of D . For larger values of D ,

$$r(D) \approx 2^{-1/3} D^{2/3} \quad (31)$$

is a reasonable approximation to Eq. (30). We conclude that the states which globally maximize the variance, for a given dimension D , can be written as

$$|\Phi_M\rangle = \frac{1}{\sqrt{r(D)}} \sum_{j=1}^{r(D)} e^{i\varphi_j} |j\rangle, \quad (32)$$

again, any shuffling of basis elements leads to a state that also maximizes the dispersion. In Fig. 4 we plot $r(D)$ between $D = 3$ and $D = 100$. The rank $r(D)$ is a slowly increasing function: for $D = 3, 4$, we find $r(D) = 2$; for $93 \leq D \leq 100$, $r(D) = 17$; and for $997 \leq D \leq 1015$ we have $r(D) = 80$. Therefore, e. g., for $D = 100$, we have $0 \leq \Delta_c \leq 0.915$. Whenever other constraints are valid, the form of the maximal states may be quite distinct from the previous equation. For instance, if one requires that the populations should coincide with the Maxwell-Boltzmann distribution (see the main text for details).

Scalability of Π and P^2

Here we demonstrate the scalability properties of purity and predictability. For $\varrho = \rho^{\otimes n}$, the purity can be written as

$$\begin{aligned}\Pi(\varrho) &= \Pi(\rho^{\otimes n}) = \sum_{\substack{i_1 \dots i_n=1 \\ j_1 \dots j_n=1}}^d |\rho_{i_1 j_1} \dots \rho_{i_n j_n}|^2 = \sum_{\substack{i_1 \dots i_n=1 \\ j_1 \dots j_n=1}}^d |\rho_{i_1 j_1}|^2 \dots |\rho_{i_n j_n}|^2 \\ &= \prod_{k=1}^n \left(\sum_{i_k, j_k}^d |\rho_{i_k j_k}|^2 \right) = \left(\sum_{i,j}^d |\rho_{ij}|^2 \right)^n = [\Pi(\rho)]^n.\end{aligned}\quad (33)$$

Now, consider the predictability

$$\begin{aligned}P^2(\varrho) &= P^2(\rho^{\otimes n}) = \sum_{i=1}^D |\varrho_{ii}|^2 - \frac{1}{D} = \sum_{i_1 \dots i_n=1}^d |\rho_{i_1 i_1} \dots \rho_{i_n i_n}|^2 - \frac{1}{d^n} = \sum_{i_1 \dots i_n=1}^d |\rho_{i_1 i_1}|^2 \dots |\rho_{i_n i_n}|^2 - \frac{1}{d^n} \\ &= \prod_{k=1}^n \left(\sum_{i_k=1}^d |\rho_{i_k i_k}|^2 \right) - \frac{1}{d^n} = \left(\sum_{i=1}^d |\rho_{ii}|^2 \right)^n - \frac{1}{d^n} = \left[P^2(\rho) + \frac{1}{d} \right]^n - \frac{1}{d^n},\end{aligned}\quad (34)$$

which finishes the demonstration.

Coherence dispersion of the partially coherent Gibbs state

Let us consider the partially coherent Gibbs state G , whose entries are

$$G_{jj} = \frac{1}{\mathcal{Z}} e^{-\beta E_j} \quad \text{and} \quad G_{jk} = \frac{\lambda}{\mathcal{Z}} e^{-\frac{\beta}{2}(E_j + E_k)} \quad (j \neq k)$$

where $\beta = (k_B T)^{-1}$ is the ‘‘reciprocal temperature’’ and $\lambda \in [0, 1]$ reflects the level of coherence of G . The purity of G is given by $\Pi = \sum_{j,k} |G_{jk}|^2$, which leads to

$$\Pi = \sum_{j,k} G_{jk}^2 = \frac{\lambda^2}{\mathcal{Z}^2(\beta)} \sum_{i,j} e^{-\beta(E_i + E_j)} + \frac{(1 - \lambda^2)}{\mathcal{Z}^2(\beta)} \sum_i e^{-2\beta E_i} = \lambda^2 + (1 - \lambda^2) \frac{\mathcal{Z}(2\beta)}{\mathcal{Z}^2(\beta)}, \quad (35)$$

where we used $|G_{jk}| = G_{jk}$ and $\mathcal{Z}(x\beta) = \sum_j e^{-x\beta E_j}$ is the system’s partition function at a temperature $T' = T/x$.

Analogously

$$P^2 = \frac{\mathcal{Z}(2\beta)}{\mathcal{Z}^2(\beta)} - \frac{1}{d} \quad \text{and} \quad C_1 = \lambda \left(\frac{\mathcal{Z}^2(\beta/2)}{\mathcal{Z}(\beta)} - 1 \right). \quad (36)$$

Therefore, the single-copy coherence dispersion reads

$$\Delta_c(G(\beta)) = \lambda^2 \left\{ \left(1 - \frac{\mathcal{Z}(2\beta)}{\mathcal{Z}^2(\beta)} \right) - \frac{1}{d^2 - d} \left(1 - \frac{\mathcal{Z}^2(\beta/2)}{\mathcal{Z}(\beta)} \right)^2 \right\}. \quad (37)$$

Now we note that

$$\frac{\mathcal{Z}(2\beta)}{\mathcal{Z}^2(\beta)} = \sum_j \frac{e^{-\beta E_j}}{\mathcal{Z}(\beta)} \cdot \frac{e^{-\beta E_j}}{\mathcal{Z}(\beta)}. \quad (38)$$

But $p_j = \frac{e^{-\beta E_j}}{\mathcal{Z}(\beta)}$ is the Maxwell-Boltzmann probability distribution. Therefore,

$$\frac{\mathcal{Z}(2\beta)}{\mathcal{Z}^2(\beta)} = \sum_j p_j^2 = \Pi_{\text{eq}}(\beta), \quad (39)$$

the purity of the thermal equilibrium state at reciprocal temperature β . Using the same reasoning we obtain

$$\left(\frac{\mathcal{Z}(\beta)}{\mathcal{Z}^2(\beta/2)} \right)^{-1} = \frac{1}{\Pi_{\text{eq}}(\beta/2)}. \quad (40)$$

Therefore

$$\begin{aligned} \Delta_c(G(\beta)) &= \lambda^2 \left[(1 - \Pi_{\text{eq}}(\beta)) - \frac{1}{d^2 - d} (1 - 1/\Pi_{\text{eq}}(\beta/2))^2 \right] \\ \Rightarrow \Delta_c(G(T)) &= \lambda^2 \left[(1 - \Pi_{\text{eq}}(T)) - \frac{1}{d^2 - d} (1 - 1/\Pi_{\text{eq}}(2T))^2 \right]. \end{aligned} \quad (41)$$

We now assume that the spectrum is that of a d -level system, given by $E_j = j\epsilon$. With this we get

$$\mathcal{Z}(\beta) = e^{-\frac{\beta}{2}(d+1)\epsilon} \frac{\sinh(\beta d\epsilon/2)}{\sinh(\beta\epsilon/2)}. \quad (42)$$

Therefore,

$$\Pi_{\text{eq}}(\beta) = \frac{\sinh(\beta d\epsilon) \sinh^2(\beta\epsilon/2)}{\sinh(\beta\epsilon) \sinh^2(\beta d\epsilon/2)} = \tanh(\beta\epsilon/2) \coth(\beta d\epsilon/2) = \tanh(2/\tau) \coth(2d/\tau), \quad (43)$$

where we defined the dimensionless temperature $\tau \equiv 4k_B T/\epsilon$. For a single copy, we obtain

$$\Delta_c(G(\tau)) = \lambda^2 (1 - \tanh(2/\tau) \coth(2d/\tau)) - \frac{\lambda^2}{d^2 - d} (1 - \coth(1/\tau) \tanh(d/\tau))^2. \quad (44)$$

Note that λ^2 is a global scale factor and, for $d = 2$, the previous expression vanishes identically, as it should.

Finally, the multi-copy coherence dispersion reads

$$\Delta_c(G^{\otimes n}(\beta)) = (\lambda^2 + (1 - \lambda^2)\Pi_{\text{eq}}(\beta))^n - \Pi_{\text{eq}}(\beta)^n - \frac{1}{d^{2n} - d^n} ((1 - \lambda + \lambda/\Pi_{\text{eq}}(\beta/2))^n - 1)^2, \quad (45)$$

which, for n d -level systems, in terms of τ , becomes

$$\begin{aligned} \Delta_c(G^{\otimes n}(\tau)) &= (\lambda^2 + (1 - \lambda^2) \tanh(2/\tau) \coth(2d/\tau))^n - (\tanh(2/\tau) \coth(2d/\tau))^n \\ &\quad - \frac{1}{d^{2n} - d^n} ((1 - \lambda + \lambda \coth(1/\tau) \tanh(d/\tau))^n - 1)^2. \end{aligned} \quad (46)$$

Note that in this expression λ^2 is no longer a simple multiplicative factor. However, since this is the case for a single copy, the maximum of the multi-copy expression above inherits a quite weak dependence on λ .

Complementary plots of Δ_c for selected values of λ , n , and d

In Fig. 3 of the main text the contour plot is too flattened in the interval $5.000 < n < 50.000$. Below we show a plot of this region only and the section corresponding to $n = 5.000$, with the peak at $\tau^* \approx 0.434$. A similar analysis was made for $n = 3 \times 10^6$, leading to $\tau^* \approx 0.257$. This, together with Eq. (5) of the main text, justify the reported interval for τ^* , i. e., $0.257 \lesssim \tau^* \lesssim 0.434$, or $-37^\circ\text{C} \lesssim T^* \lesssim 125^\circ\text{C}$.

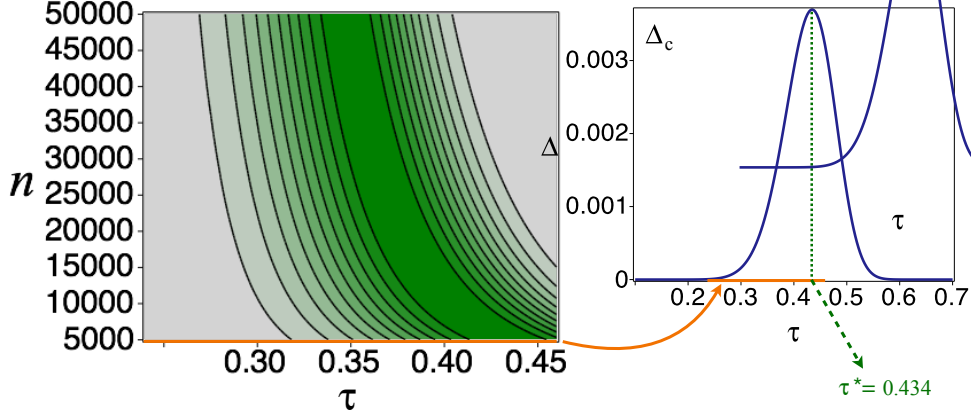


FIG. 5: Plot of Δ_c as a function of n and the dimensionless temperature τ , for n ranging from 5.000 to 50.000 and $\lambda = 0.1$. Δ_c vanishes in the light gray regions and the green stripe marks the locus of the maxima. The section $n = 5.000$ is also shown (the orange line corresponds to the horizontal interval in the contour plot).

Next, we illustrate the fact that the temperature interval is largely independent of the dimension d , that is, assuming that the ECSs are two-level systems is not essential to obtain the reported results. In Fig. 3 we plot Δ_c as a function of n and τ for n ranging from 3×10^5 to 8×10^5 and $\lambda = 0.1$. In the left panel we use $d = 2$, whereas in the right panel we set $d = 20$. The contours are essentially identical.

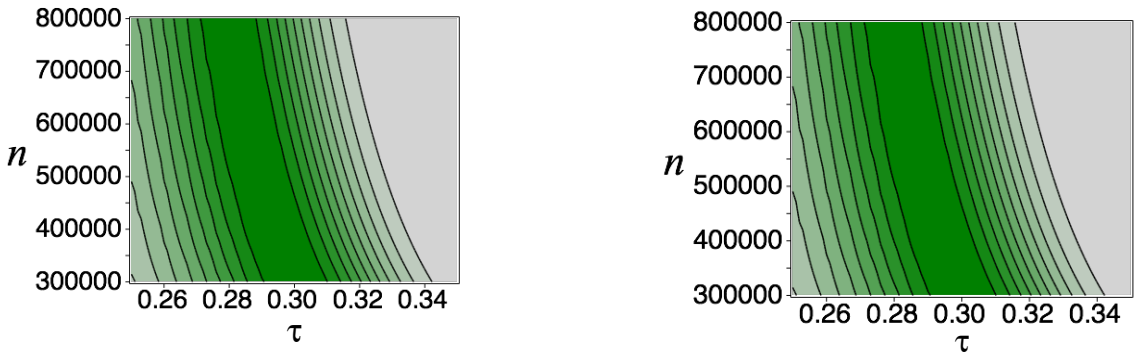


FIG. 6: Contour plot of Δ_c as a function of n and the dimensionless temperature τ , for n ranging from 3×10^5 to 8×10^5 for $\lambda = 0.1$. In the left panel we set $d = 2$ and in the right panel we used $d = 20$. The two plots are indistinguishable to the eye.

For quite small numbers, the dimension does make some difference, as illustrated in Fig. 4, where the only modification with respect to the previous figure is the range $3 < n < 50$. Small differences can be observed. Now we address the effect of varying λ . Despite the variation in the peak intensity, in the four figures below we illustrate the fact that the position τ^* of maximum coherence dispersion is essentially independent of λ , for a wide range of values of λ . For $\lambda = 0.01$ and $d = 2$, with $5000 < n < 3 \times 10^6$ we obtain that maximal dispersion covers the τ^* -interval $[0.257, 0.435]$, while for $\lambda = 0.5$ and $d = 2$, with $5000 < n < 3 \times 10^6$ we obtain that maximal dispersion covers the τ^* -interval $[0.259, 0.441]$. So, the variation of the coherence level by a factor of 50, leaves the temperature intervals for which Δ_c is maximized almost unchanged.

The general conclusion is: for numbers $n > 50$ and a wide range of values of λ and d , the position of the maximum coherence dispersion slowly depends on n , varying by a factor of ~ 2 as n goes from a few thousands to three millions. The temperature intervals are largely insensitive to variations of d and λ .

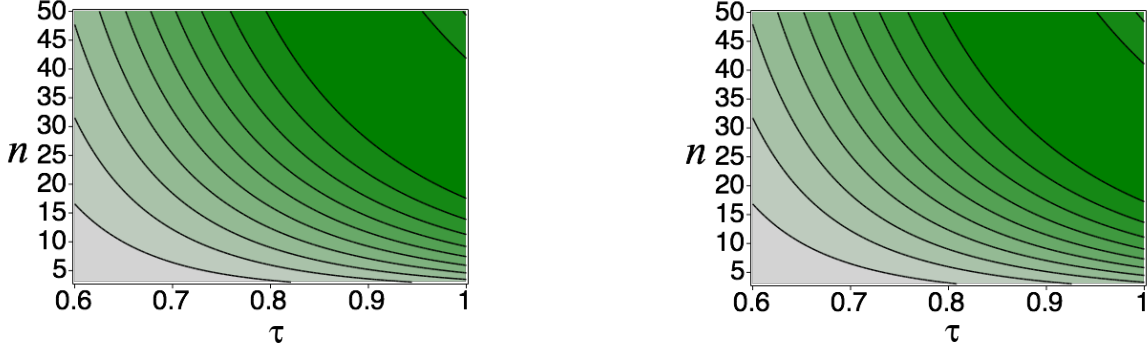


FIG. 7: Contour plot of Δ_c as a function of n and the dimensionless temperature τ , for n ranging from 3 to 50 for $\lambda = 0.1$. In the left panel we set $d = 2$ and in the right panel we used $d = 20$. A small difference shows up in the upper-right regions and around $n = 3$.

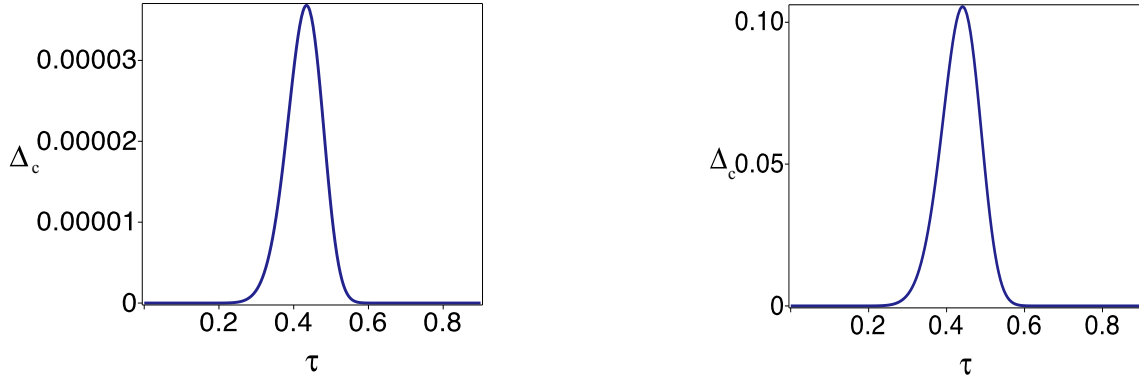


FIG. 8: In the left panel we have $\lambda = 0.01$ and in the right panel we set $\lambda = 0.5$. From left to right, the value of τ^* goes from 0.435 to 0.441. In both cases we used $n = 5000$ and $d = 2$. The temperature for which maximum variability is attained is essentially independent of λ . In both cases we used $n = 3 \times 10^6$ and $d = 2$.

Considering the “incoherent buffer”

One may ask about the effect of the incoherent (thermal) fraction of energy consumption sites (ECSs) on Δ_c , since it is not reasonable to assume that all ECS within a cell present a non-vanishing coherence content, at any moment. Here, we explicitly consider this point. Let N be the total number of ECSs and n the number of ECSs with coherence level λ . So that the full state of the set of ECSs is given by:

$$G^{\otimes n} \otimes \rho_G^{\otimes (N-n)}, \quad (47)$$

where ρ_G denotes the thermal equilibrium Gibbs state. Using arguments similar to those of section III of this supplemental material one can easily show that:

$$\Delta_c(G^{\otimes n} \otimes \rho_G^{\otimes (N-n)}) = \Pi(G)^n \Pi(\rho_G)^{N-n} - \left(P(G)^2 + \frac{1}{d} \right)^N - \frac{[(1 + C_1(G))^n - 1]^2}{d^{2N} - d^N}, \quad (48)$$

where we used $P^2(G) = P^2(\rho_G)$ and $C_1(\rho_G) = 0$. This leads to

$$\Delta_c(G^{\otimes n} \otimes \rho_G^{\otimes (N-n)}) = \Pi_{\text{eq}}(\tau)^{N-n} \left[(\lambda^2 + (1 - \lambda^2) \Pi_{\text{eq}}(\tau))^n - \Pi_{\text{eq}}(\tau)^n \right] - \frac{1}{d^{2N} - d^N} ((1 - \lambda + \lambda/\Pi_{\text{eq}}(2\tau))^n - 1)^2,$$

where $\tau \equiv 4k_B T/\epsilon$ and $\Pi_{\text{eq}}(\tau) = \tanh(2/\tau) \coth(2d/\tau)$.

We checked that the insensitivity of the temperature interval against variations of d and λ is also present here. By proceeding the same inferences as in the main text, we find a temperature interval, with limiting values which differ

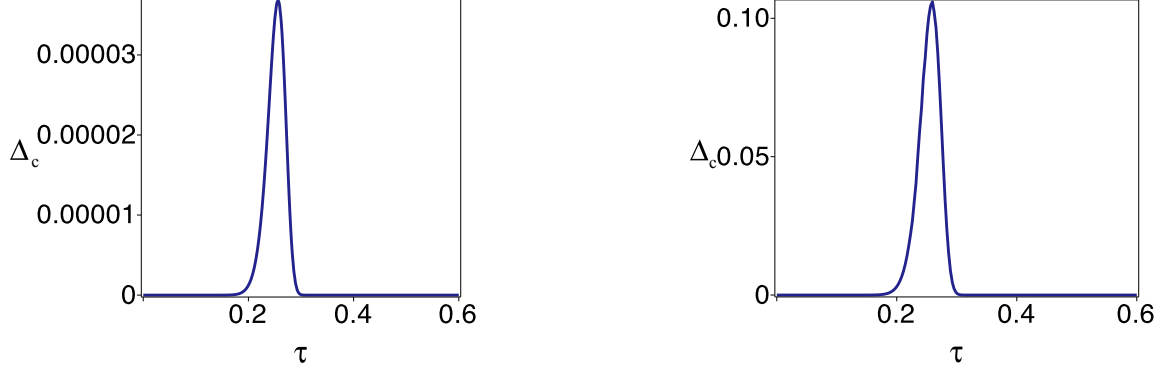


FIG. 9: The same as the previous figure with $n = 3 \times 10^6$. In the left panel we have $\lambda = 0.01$ and in the right panel we set $\lambda = 0.5$. From left to right, the value of τ^* goes from 0.257 to 0.259. Again, the temperature for which maximum variability is attained is essentially independent of λ .

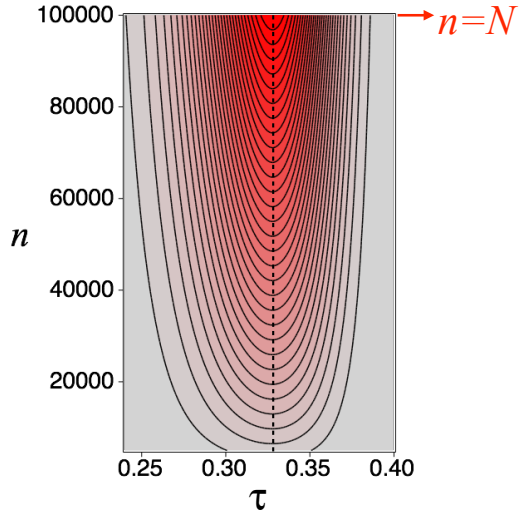


FIG. 10: Contour plot of Δ_c as a function of τ and n for $N = 10^6$ and $\lambda = 0.1$. As n grows, for fixed N , the position τ^* of the maximum does not change. Of course, the intensity of the maximum grows as N/n drops.

from those of Eq. (6) of the main text by less than 1%. The clearest way to understand why this is so, is by inspecting a contour plot of Δ_c against τ and n , for fixed N , keeping in mind that the present model and its simpler version (in the main text), coincide whenever $N = n$. This plot is shown in Fig. 10, where the constancy of τ^* is evident. Since the models coincide for $n = N$, we conclude that the maxima of both models occur for the same temperatures.

The question arises, how does the temperature interval emerges? The fact is that in the simple model, only n is considered, but in the present model, what makes the temperature τ^* slowly change is N , rather than n . In Fig. 11, we plot Δ_c against τ and N , for fixed n . We checked that the locus of the maxima is essentially unchanged with respect to the simpler model of the main text. We conclude that the incoherent fraction of ECSSs does not change our main conclusions.

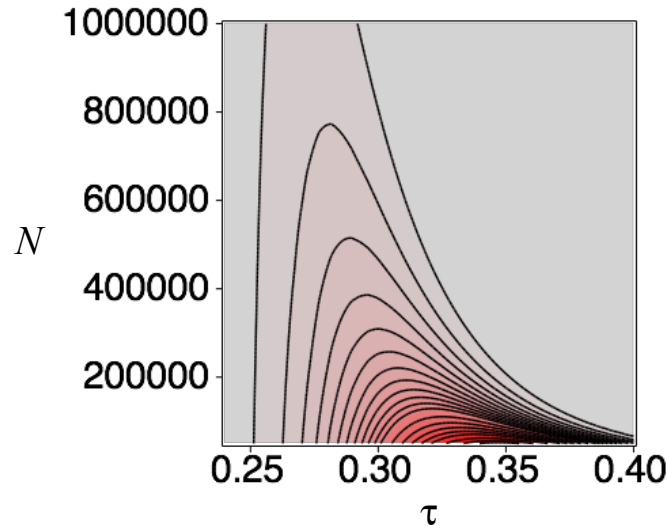


FIG. 11: Contour plot of Δ_c as a function of τ and N (the total number of ECSs) for $n = 50.000$ and $\lambda = 0.1$. To facilitate visualization we limited the horizontal range to $50.000 \leq N \leq 10^6$. As N grows, for fixed n , the maximum intensity drops.